Functional brain mapping with locally smoothed regression

Conference Paper *in* Proceedings / IEEE International Symposium on Biomedical Imaging: from nano to macro. IEEE International Symposium on Biomedical Imaging · April 2013

DOI: 10.1109/ISBI.2013.6556820

6 authors, including:

Jiangang Liu

87 PUBLICATIONS **787** CITATIONS

SEE PROFILE

Wenjuan Wei

Chinese Academy of Sciences

13 PUBLICATIONS **98** CITATIONS

SEE PROFILE

Jie Tian

Chinese Academy of Sciences

661 PUBLICATIONS **7,114** CITATIONS

SEE PROFILE

Kang Lee

University of Toronto

301 PUBLICATIONS **6,947** CITATIONS

SEE PROFILE

FUNCTIONAL BRAIN MAPPING WITH LOCALLY SMOOTHED REGRESSION

Lu Feng[1], Jiangang Liu[2], Ling Li[2], Wenjuan Wei[1], Jie Tian[1, 3*], IEEE Fellow, Kang Lee[4, 5*]*

[1] Institute of Automation, Chinese Academy of Sciences, Beijing, 100190, China
[2] School of Computer and Information Technology, Beijing Jiaotong University, Beijing, 100044, China
[3] School of Life Sciences and Technology, Xidian University, Shaanxi, 710071, China
[4] Dr. Eric Jackman Institute of Child Study, University of Toronto, Toronto, Ontario, Canada
[5] Department of Psychology, University of California, San Diego, La Jolla, California, USA
tian@ieee.org; kang.lee@utoronto.ca; liujg@bjtu.edu.cn

ABSTRACT

High-resolution functional magnetic resonance imaging (hi-res fMRI) methodology offers an opportunity for neuroscientists to gain insight about brain activities at a finer scale, and is thus becoming increasingly common. Traditional voxel-wise general linear model (GLM) is not suitable for hi-res functional brain mapping because local averaging may lose valuable fine-grained information boasted by hi-res fMRI. The searchlight approach may be more suited for this situation, but it can be improved to integrate multi-voxel information more completely and effectively. We propose a locally smoothed regression (LSR) to find the spatial organizations of neural activities, especially for hi-res data. LSR is a flexible model whereby the traditional voxel-wise regression can be seen as a special case of LSR. Further, LSR can be integrated into Mahalanobis-distance-based searchlight framework. This new approach promises to provide improved and reliable activation mapping as illustrated here by applying it to analyze a real set of data using hi-res fMRI imaging.

Index Terms — High-resolution functional magnetic resonance imaging, Multivariate pattern analysis, Searchlight approach, Brain activation localization

1. INTRODUCTION

With the improvement of fMRI technology, brain activity can be measured at a higher spatial resolution. Nowadays, the spatial resolution of standard fMRI is about $4 \times 4 \times 4\ mm^3$. Using widely-available 3-Tesla MR scanners, hi-res functional measurements are robustly achievable with a resolution of $2 \times 2 \times 2\ mm^3$. If we use a higher magnetic field (> 3T) or parallel scanning technology, a spatial resolution in the sub-millimeter range can be achieved [1]. Hi-res fMRI offers fine-grained spatial information of neural activity, and make it possible to ask certain research questions that could not be directly addressed previous. For instance, previous studies using the standard fMRI methods revealed a face-preferential region in the ventral tempo-occipital cortex, commonly referred to as the fusiform face area (FFA) [2], and triggered a debate about the structure and function of this region. A hi-res fMRI study suggested the FFA is a heterogeneous module which contains non-face-selective clusters interdigitated with face-selective clusters [3].

Traditional single-voxel-based pipeline for functional brain mapping is not suited for hi-res fMRI data, because it depends on spatial smoothing with a 4-8 mm FWHM Gaussian kernel. Spatial blurring obscures valuable fine-grained information boasted by hi-res fMRI. However, we cannot omit smoothing directly, due to its crucial role in GLM. First, smoothing enhances functional contrast-to-noise ratio (FCNR). Second, GLM assumes the error terms are normally distributed, and Gaussian smoothing can achieve greater validity of the statistical assumption [4]. If smoothing is omitted, a brain activation map with salt-and-pepper patterns is generated instead of a blob-like activation map [5]. After setting a statistical threshold, we will obtain some scattered tiny activated regions, and can even not tell experimental effects from noises (Fig. 1). Additionally, whereas hi-res fMRIs achieve higher spatial resolutions, it loses FCNR as a price [1]. That makes omitting of smoothing inadvisable.

In order to solve this problem, some wavelet-based statistical analysis methods have been proposed where the Gaussian prefilter in GLM is replaced by a spatial wavelet transform (i.e. [6]). However, this method lacks a statistical interpretation in the spatial domain. The more recent searchlight approach is a spatial-domain method and is also applied to unsmoothed data [5]. The essential ideas of searchlight are as following: (1) taking into consideration all the neighboring voxels fallen within the scope of the searchlight (traditional voxel-wise GLM considers only one voxel at a time); (2) solving a problem of multivariate multiple linear regression (traditional voxel-wise GLM solves a problem of univariate multiple linear regression); (3) using the Mahalanobis distance as a measurement of difference between effects of two experimental conditions (traditional voxel-wise GLM uses Euclidean distance to measure such difference). However, the searchlight approach fails to integrate multi-voxel information thoroughly. It uses least squares methods to solve the problem of multivariate multiple linear regression, whereby all the voxels within searchlight are used simultaneously. In fact, this un-regularized optimization is equivalent to the voxel-wise multiple linear regression (i.e. without any constraint, the jointly regression of multiple voxels is equivalent to multiple single voxel regressions).

Here, we propose a novel, locally smoothed regression (LSR) method to generate function brain mappings, especially for hi-res data. The LSR also applies to unsmoothed data. A regularized optimization is used here instead of the un-regularized optimization in the searchlight approach. Specially, the neighboring voxels are used as a smoothness regularization to guarantee the accurate estimation of the regression for the current voxel. In addition, a Gaussian weight coefficient is introduced to simulate different effects of neighboring voxels at different distances. LSR is a flexible framework which has two hyper-parameters α and β. By tuning these two parameters, LSR can be adjusted smoothly to different level of regularization. Furthermore, by setting specific

values for α and β, the LSR can be transformed into the voxel-wise regression or Gaussian-smoothness-based GLM. Additionally, we can directly conduct statistical tests on regression coefficients, or compute the Mahalanobis distances between regression coefficients of two different predictors before a statistical test. We compared the results of the LSR with those of GLM and the searchlight approach on a set of hi-res real fMRI data, and found the LSR is more powerful than GLM and the searchlight approach.

2. METHODS

2.1. Proposed: Locally Smoothed Regression

Supposing N functional images are acquired consecutively, and each image contains M voxels. The time sequence of voxel i is denoted as $y_i \in R^N$, $i = 1, \cdots, M$. We construct a spherical searchlight of radius r, and move its center from voxel 1 to voxel M in turn. $X \in R^{N \times P}$ is the design matrix with P predictors. As those in GLM, predictors here represent a hemodynamic response for each condition, head-motion effects, and session effects. $b_i \in R^P$ denotes the basis weight for voxel i, $i = 1, \cdots, M$.

When the searchlight is centered at voxel i, all the neighboring voxels fallen within the searchlight are taken into consideration to estimate b_i simultaneously. The objective function is as following:

$$\min_{b_i, \xi_j} \|y_i - Xb_i\|^2 + \beta \sum_{\substack{j \in NN(i) \\ j \neq i}} f_j \left[\left\| y_j - X(b_i + \xi_j) \right\|^2 + \alpha \|\xi_j\|^2 \right]$$

where the first term is the traditional GLM on voxel i and the second term is a regularization of smoothness among the neighborhood voxels. The $NN(i)$ represents the nearest neighborhood of voxel i. We call this model the locally smoothed regression (LSR). In LSR, the local information (neighborhood voxels) is used to guarantee an accurate estimation of the regression coefficient for voxel i. We suppose the neighborhood voxel j to have a regression bias as $b_i + \xi_j$, where $\xi_j \in R^P$ is a slack variable for voxel j and is supposed to be as small as possible. That means the regression results of neighborhood voxels can be different from that of voxel i, but we want to minimize these differences. $f_j < 1$ is a Gaussian weight coefficient of voxel j. This term attenuates the effect of a neighboring voxel when it's getting far away from voxel i, and the weight of voxel i is set to maximum value 1.

The LSR is a convex quadratic optimization problem which has a closed-form solution as following:

$$b_i = \left((\bar{f}\beta + 1) X^T X - \bar{f}\beta X^T X A X \right)^{-1} X^T (y_i + \beta \bar{y} - \beta X A \bar{y})$$

where

$$A = (X^T X + \alpha I)^{-1} X^T$$

$$\bar{y} = \sum_{\substack{j \in NN(i) \\ j \neq i}} f_j y_j \qquad \bar{f} = \sum_{\substack{j \in NN(i) \\ j \neq i}} f_j$$

We use two hyper-parameters α and β to make LSR a general framework covering GLM with or without Gaussian smoothing as special cases. The α is used to constrain the difference between the regression coefficient of neighborhood voxel j and that of the current voxel i. The larger α is, the closer the regression results of the neighborhood voxels will be. The β changes the amount of the influence from the whole neighborhood. When setting $\beta = 0$, we can see the result becomes

$$b_i = (X^T X)^{-1} X^T y_i$$

In this case, LSR is degenerated into the single-voxel regression. Also, we can tune β to achieve different degrees of smoothing effect. When setting $\alpha = +\infty$ and $\beta = 1$, the result becomes

$$b_i = \left((\bar{f} + 1) X^T X \right)^{-1} X^T (y_i + \bar{y})$$

This is equivalent to GLM with Gaussian smoothing (i.e. using $\frac{y_i + \bar{y}}{\bar{f} + 1}$ for regression).

From the analysis above, we can find that LSR is a general model, and we can tune the values of α and β to achieve different levels of smoothness (from single-voxel regression to GLM with Gaussian smoothing).

2.2. Model Evaluation

Supposing $c \in R^P$ is the contrast vector, which represents the comparison between different predictors. Then $c^T b_i$ is the result of comparison and can be used to measure the contribution of voxel i in the condition-specific effect. Supposing $B \in R^{P \times M}$ denotes the coefficient matrix for the whole brain, $c^T B$ is the condition-specific brain mapping. To compare maps of different participants, we transform $c^T B$ into a Z-map, namely a normal distribution. Numerical methods (i.e. the randomization test used in [5]) can also be used here, although they are much more time consuming.

Alternatively, we can integrate the LSR into the Mahalanobis-distance-based framework. Supposing $Y_s \in R^{N \times L}$ is the time sequences of voxels within the searchlight, where L is the number of voxels within the searchlight. $B_s \in R^{P \times L}$ is the basis weights of voxels within the searchlight. Then the Mahalanobis distance is defined as

$$\Delta^2 = a \Sigma^{-1} a^T$$

$$a = c^T B_s$$

$$\Sigma = E^T E \qquad E = Y_s - X B_s$$

A statistical test is followed, and a Z-map can be obtained.

We use z_i to denote the value of voxel i in the Z-map. Then z_i is the activated intensity of voxel i. When a threshold z_{thresh} is set and $z_i > z_{thresh}$ is satisfied, voxel i is a supra-threshold voxel. All the adjacent supra-threshold voxels constitute a supra-threshold cluster. Supposing in total there are V supra-threshold voxels and C supra-threshold clusters, then the averaged volume of supra-threshold cluster is $\bar{V} = \frac{V}{C}$, and we use $\bar{V}$ to describe the degree of clustering.

Two standards are used here to evaluate the effect of mapping, one is the degree of clustering $\bar{V}$, and the other is the activated intensity or reliability z_i. Hyper-parameters α and β can be determined by nested cross validation to maximum $\bar{V}$ and z_i.

3. RESULTS

3.1. Experimental Design and Preprocessing

We obtained a set of hi-res fMRI data from ten adults (four males, six females, averaged age 22) recorded in a localizer experiment designed to map face-preferential regions. During the experiment, 8 20-s blocks of face images and 8 20-s blocks of common object images were presented alternately. Participants were asked to simply view two kinds of images and complete a one-back task just like previous studies [7]. For each participant, we acquired 288 21-slice echo-planar-imaging (EPI) scans lasting 2 s each. Each EPI scan had an in-plane resolution of $2 \times 2\ mm^2$ and a slice thickness of $2\ mm$ with $0.2\ mm$ gap. We also acquired a coplanar anatomical image before EPI scanning to overlap the functional

mapping onto it. The coplanar anatomical image had an in-plane resolution of $1 \times 1\, mm^2$ and a slice thickness of $2\, mm$ with $0.2\, mm$ gap. The whole tempo-occipital cortex was covered using a scanning plane paralleled to the proximal surface between cerebrum and cerebellum.

The first three volumes of each session were discarded due to T1 effects. The remaining volumes were slice-time corrected, realigned to the first volume of the first session, session-effect removed, and high-pass filtered to remove the scanner drift and low-frequency artifacts. The data were smoothed for GLM using a $6 \times 6 \times 6\, mm^3$ FWHM Gaussian kernel, but unsmoothed for the searchlight approach and LSR. We used a 6-mm-radius searchlight in both the searchlight approach and LSR, and a $6 \times 6 \times 6\, mm^3$ FWHM Gaussian kernel to compute the Gaussian weight coefficients in LSR.

3.2. Results of LSR

We compared the function brain mapping generated by the LSR with those created by other methods, and found that the LSR-based map highlighted some regions not covered by the GLM-based map or searchlight-based map (see slice 3 in Fig. 1). As mentioned above, the GLM without smoothing only generated scattered salt-and-pepper activation maps (Fig. 1(A)). The GLM with smoothing revealed several expected activation regions, as well as several less task-related activations which were difficult to explain (Fig. 1(B)). The searchlight-based map was more concentrated (Fig. 1(C)). It highlighted regions whose activity pattern was specifically important to distinguish two categories (face/object), and extended to surrounding areas. However, it missed the activation in the right superior temporal sulcus (STS). The LSR-based map showed activations in the face-preferential regions, the right FFA and right STS [8], as well as activations in the primary visual cortex (Fig. 1(D)). Looking inside these face-preferential regions, we found that the difference between the neural activities of face-viewing and those of object-viewing was greater when LSR was used compared to that when the GLM or the searchlight approach was used. Further, neural activities induced by face-viewing within the face-preferential areas detected by LSR were stronger than those within face-preferential regions revealed by GLM or the searchlight approach (Fig. 1).

When different hyper-parameters α and β are set, different levels of smoothness can be achieved. We plotted the degree of clustering $\bar{V}$ as a function of α and β, and found that different participants had different optimized combinations of α and β (Fig. 2). The reason why LSR outperformed the Gaussian-smoothness-based GLM might be that LSR took into consideration all the possible combinations of α and β in addition to the special case of $\alpha = +\infty$ and $\beta = 1$ which was equivalent to the Gaussian-smoothness-based GLM.

Compared to the searchlight-based map, the LSR-based map had more overlap with the map of Gaussian-smoothness-based GLM (Fig. 3). A probable explanation is that the Mahalanobis distance is an undirected measure which can measure how great the difference between effects of two conditions is, but cannot indicate which condition dominates in this difference. Thus, the searchlight-based map involves a part of activations induced by object-viewing compared to face-viewing. In addition, brain regions whose responses are greater to object images than that to face images are adjacent to the face-preferential regions [9], and may connect with face-preferential regions to form a large cluster.

We integrated the LSR into the Mahalanobis-distance-based framework, and found that the new method was more sensitive than the searchlight approach. Although these two methods both used an undirected measure, the Mahalanobis distance, to compute the difference between effects of two experimental conditions, the new approach outperformed the searchlight approach by finding the bilateral FFAs of all ten participants (Fig. 4 (a)). Additionally, the new approach detected the bilateral occipital face areas (OFAs) whose areas were much larger than those detected by the searchlight approach (Fig. 4(b)).

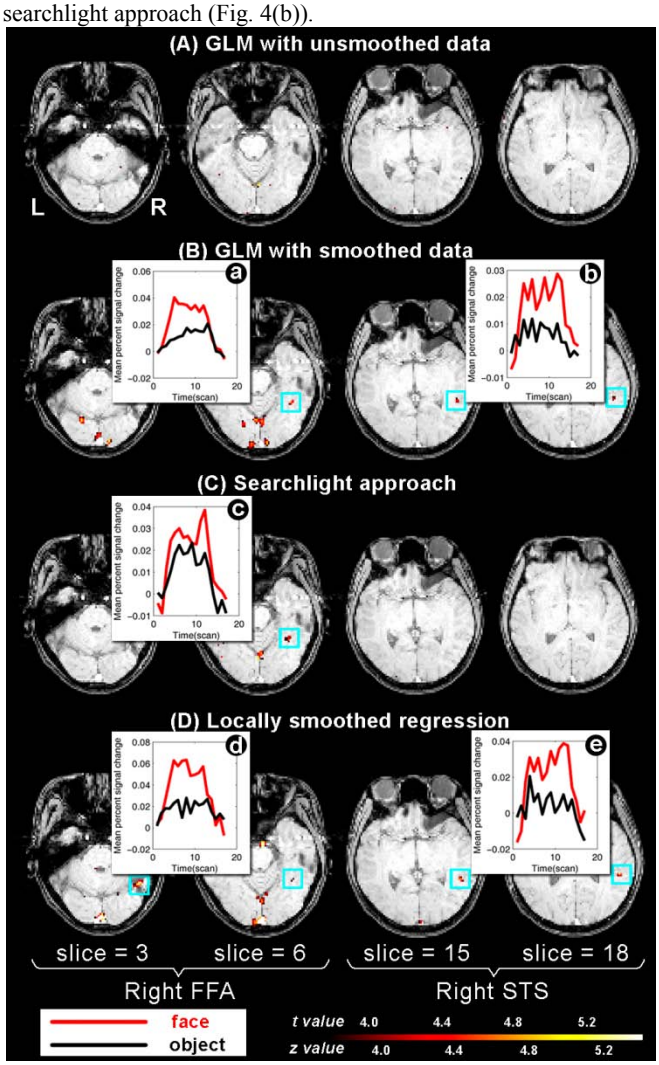

Fig. 1. Functional brain mapping of one participant using (A) general linear model (GLM) with unsmoothed data, (B) GLM with smoothed data, (C) searchlight approach, and (D) locally smoothed regression (LSR). Activation maps are overlapped onto the coplanar anatomical image of this participant. Blue squares indicate the face-preferential regions, the right fusiform face area (FFA) on the left two slices and the right superior temporal sulcus (STS) on the right two slices. Activation maps are generated by a uniform threshold of $p < 0.0001$. Line plots which floating on the top show the mean time courses of percent fMRI signal change within (a) the right FFA detected by GLM with smoothing, (b) right STS detected by GLM with smoothing, (c) right FFA detected by searchlight approach, (d) right FFA detected by LSR, and (e) right STS detected by LSR. Red line is the time course of face block, and black line is the time course of object block.

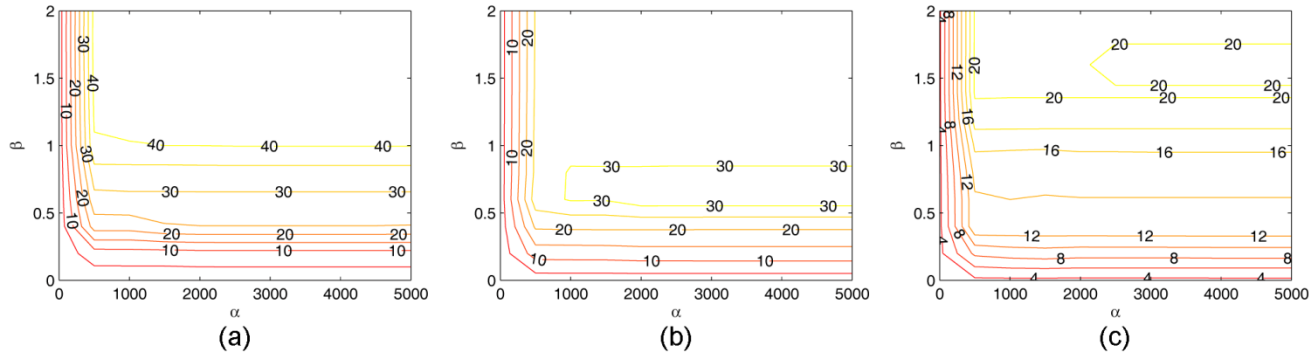

Fig. 2. The contour plots demonstrate the degree of clustering $\bar{V}$ as a function of hyper-parameters α and β. The contour labels show the value of $\bar{V}$. Three contour plots belong to three representative participants.

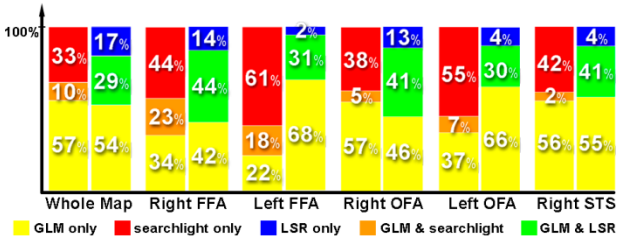

Fig. 3. Proportion of voxel sets and their intersection averaged across all 10 participants. The results are calculated within the whole brain map, the right fusiform face area (FFA), the left FFA, the right occipital face area (OFA), the left OFA, and the right superior temporal sulcus (STS) respectively. Notice that GLM here represents the Gaussian-smoothness-based GLM.

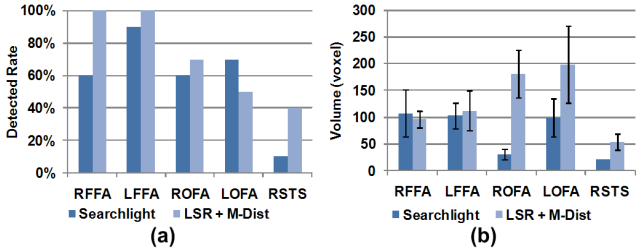

Fig. 4. Comparison of performances of the searchlight approach (abbr. as searchlight) and the LSR integrated into Mahalanobis-distance-based searchlight framework (abbr. as LSR + M-Dist). (a) Detected rates of different regions of interest (ROIs) on ten participants. (b) Mean volume of each ROI detected by two methods respectively with their SEMs. RFFA = right fusiform face area; LFFA = left fusiform face area; ROFA = right occipital face area; LOFA = left fusiform face area; RSTS = right superior temporal sulcus.

4. DISCUSSIONS AND CONCLUSIONS

We propose a locally smoothed regression which uses multi-voxel information to implement a functional brain mapping. The proposed method is a flexible model which includes the single-voxel regression and Gaussian-smoothness-based GLM as special cases. Additionally, the LSR can be integrated into the searchlight framework by calculating the Mahalanobis distance between coefficients after regression. By tuning the hyper-parameters α and β, different levels of smoothness can be achieved (e.g. smoothed and non-smoothed GLM), and therefore, a much more flexible and accurate human brain mapping result can be found with the LSR.

5. ACKNOWLEDGEMENTS

This paper is supported by the National Basic Research Program of China (973 Program) under Grant 2011CB707700, the National Natural Science Foundation of China under Grant No. 81227901, 61231004, 30970771, 60910006, 31028010, 30970769, the Fundamental Research Funds for the Central Universities (2011JBM226) and NIH (R01HD046526 & R01HD060595).

6. REFERENCES

[1] N. Kriegeskorte, and P. Bandettini, "Analyzing for information, not activation, to exploit high-resolution fMRI," *Neuroimage*, vol. 38, no. 4, pp. 649-662, 2007.

[2] N. Kanwisher, J. McDermott, and M.M. Chun, "The fusiform face area: a module in human extrastriate cortex specialized for face perception," *The Journal of Neuroscience*, vol. 17, no. 11, pp. 4302-4311, 1997.

[3] K. Grill-Spector, R. Sayres, and D. Ress, "High-resolution imaging reveals highly selective nonface clusters in the fusiform face area," *Nature Neuroscience*, vol. 9, no. 9, pp. 1177-1185, 2006.

[4] K.J. Friston, et al., "Statistical parametric maps in functional imaging: A general linear approach," *Human Brain Mapping*, vol. 2, no. 2, pp. 189-210, 1995.

[5] N. Kriegeskorte, R. Goebel, and P. Bandettini, "Information-based functional brain mapping," *Proceedings of the National Academy of Sciences of the USA*, vol. 103, no. 10, pp. 3863-3868, 2006.

[6] U.E. Ruttimann, et al., "Statistical analysis of functional MRI data in the wavelet domain," *IEEE Transactions on Medical Imaging*, vol. 17, no. 2, pp. 142-154, 1998.

[7] L. Feng, et al., "The other face of the other-race effect: An fMRI investigation of the other-race face categorization advantage," *Neuropsychologia*, vol. 49, no. 13, pp. 3739-3749, 2011.

[8] J.V. Haxby, E.A. Hoffman, and M.I. Gobbini, "The distributed human neural system for face perception," *Trends in Cognitive Sciences*, vol. 4, no. 6, pp. 223-233, 2000.

[9] A. Ishai, et al., "The representation of objects in the human occipital and temporal cortex," *Journal of Cognitive Neuroscience*, vol. 12, suppl. 2, pp. 35-51, 2000.